

## Electronic Supporting Information

### **Perovskite-type Stabilizer for Efficient and Stable Formamidinium-based Lead Iodide Perovskite Solar Cells**

Lina Shen<sup>#</sup>, Peiquan Song<sup>#</sup>, Lingfang Zheng<sup>#</sup>, Kaikai Liu, Kebin Lin, Wanjia Tian, Yujie Luo, Chengbo Tian, Liqiang Xie<sup>\*</sup>, and Zhanhua Wei<sup>\*</sup>

Xiamen Key Laboratory of Optoelectronic Materials and Advanced Manufacturing,  
Institute of Luminescent Materials and Information Displays, College of Materials  
Science and Engineering, Huaqiao University, Xiamen 361021, China.

E-mail: [lqxie@hqu.edu.cn](mailto:lqxie@hqu.edu.cn), [weizhanhua@hqu.edu.cn](mailto:weizhanhua@hqu.edu.cn)

<sup>#</sup> These authors contributed equally to this work.

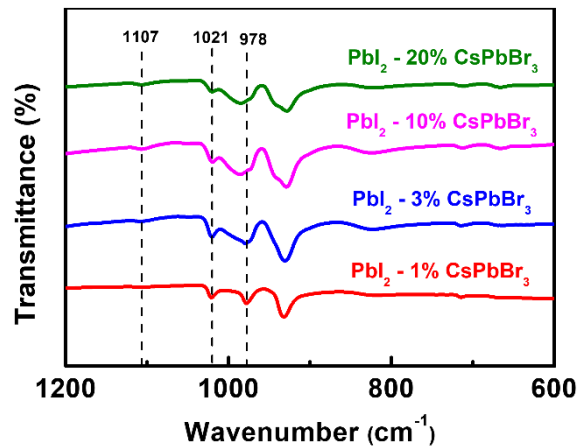


Figure S1. FTIR spectra of  $\text{PbI}_2$  films with  $\text{CsPbBr}_3$ . The doping percentage of  $\text{CsPbBr}_3$  is defined by the molar percentage of lead.

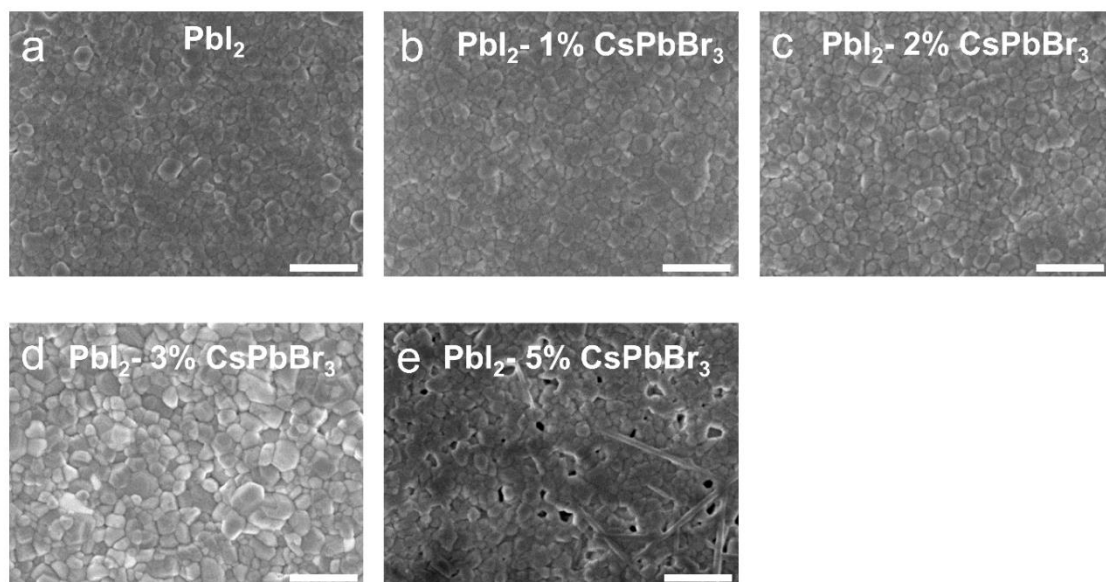


Figure S2. Top-view SEM images of  $\text{PbI}_2$  films a) w/o, b) with 1%, c) with 2%, d) with 3%, and e) with 5%  $\text{CsPbBr}_3$ . Scale bar in a) b) c) d) e) represents 500 nm.

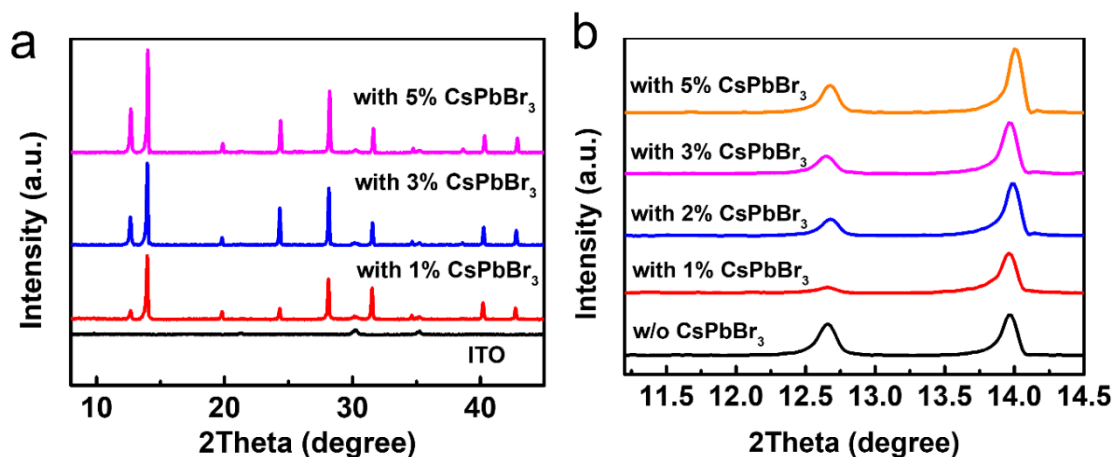


Figure S3. a) XRD patterns of FAPbI<sub>3</sub>-based perovskite films stabilized with CsPbBr<sub>3</sub>. b) Evolution of XRD peak intensity at around 12.7 and 14° of the perovskite films w/o and with CsPbBr<sub>3</sub>. The samples are deposited on ITO.

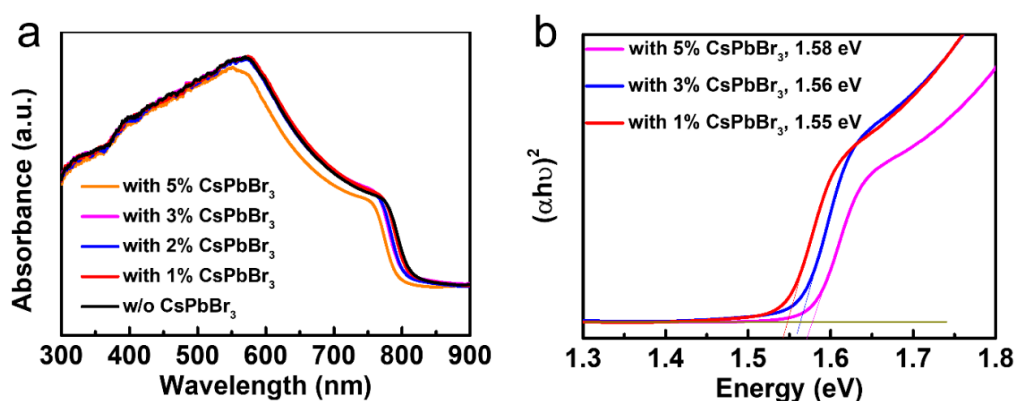


Figure S4. a) UV-vis absorption spectra of FAPbI<sub>3</sub>-based perovskite films w/o and with CsPbBr<sub>3</sub>. b) Tauc plot of perovskite films with CsPbBr<sub>3</sub>.

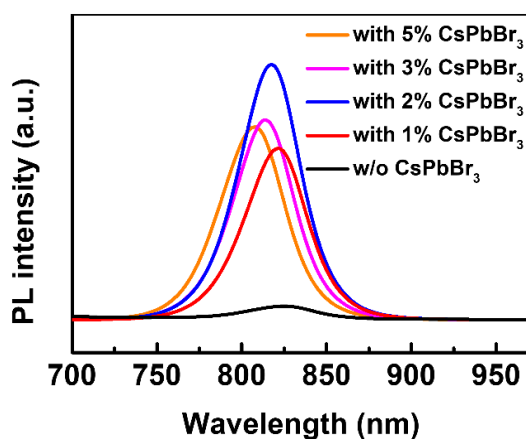


Figure S5. Steady-state PL spectra of FAPbI<sub>3</sub>-based perovskite films w/o and with CsPbBr<sub>3</sub>.

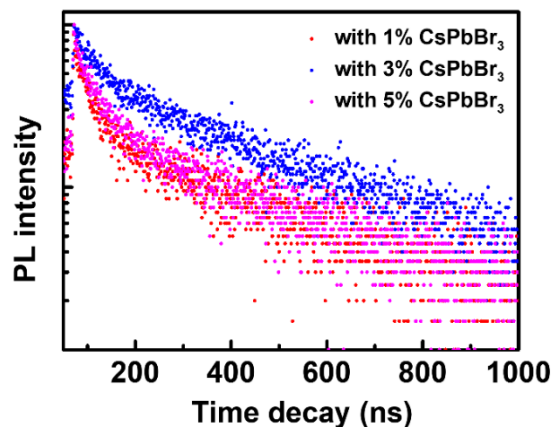


Figure S6. TRPL decay of FAPbI<sub>3</sub>-based perovskite films with CsPbBr<sub>3</sub>.

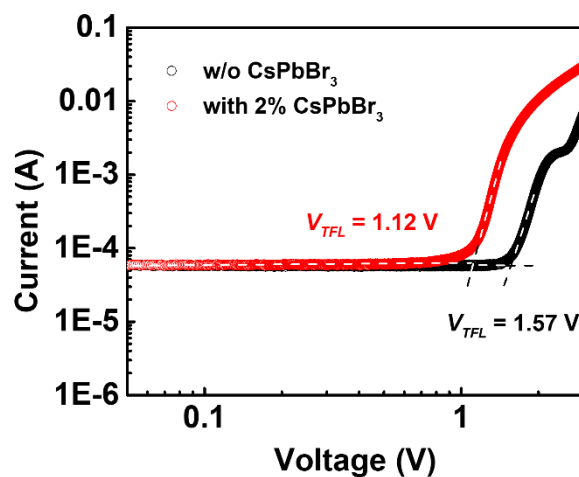


Figure S7. SCLC results of the FAPbI<sub>3</sub>-based devices w/o and with CsPbBr<sub>3</sub>. To calculate the trap density, the thickness of both perovskites is determined to be 680 nm by cross-sectional SEM and the employed dielectric constant  $\epsilon$  is 46.9 (ref. 21).

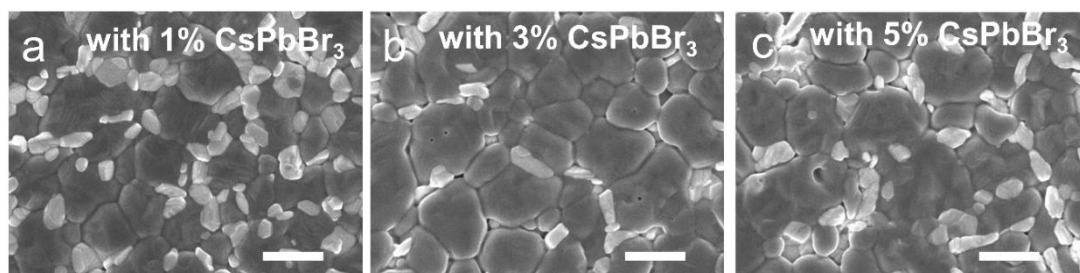


Figure S8. Top-view SEM images of FAPbI<sub>3</sub>-based perovskite films a) with 1%, b) with 3%, c) with 5% CsPbBr<sub>3</sub>. Scale bar in a) b) c) represents 1  $\mu$ m.

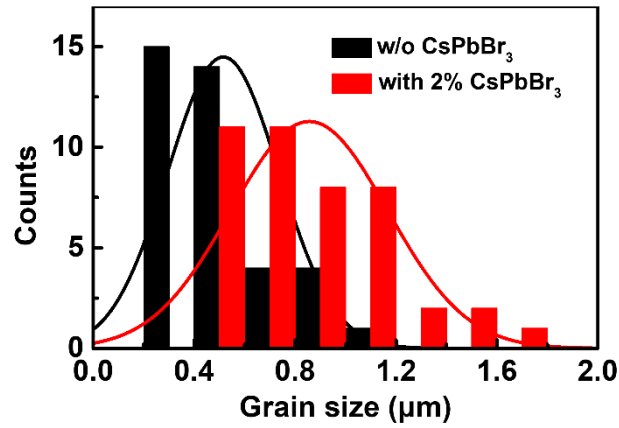


Figure S9. Grain-size distribution of the FAPbI<sub>3</sub>-based perovskite films w/o and with 2% CsPbBr<sub>3</sub>.

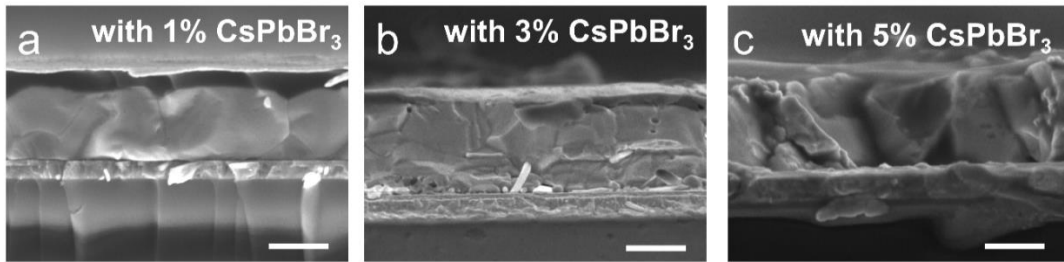


Figure S10. Cross-sectional SEM images of FAPbI<sub>3</sub>-based PSCs a) with 1%, b) with 3%, c) with 5% CsPbBr<sub>3</sub>. Scale bar in a) b) c) represents 500 nm.

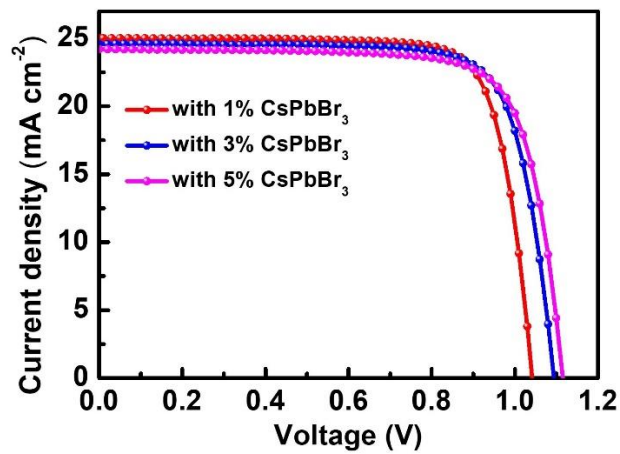


Figure S11.  $J$ - $V$  curves of FAPbI<sub>3</sub>-based PSCs with CsPbBr<sub>3</sub>.

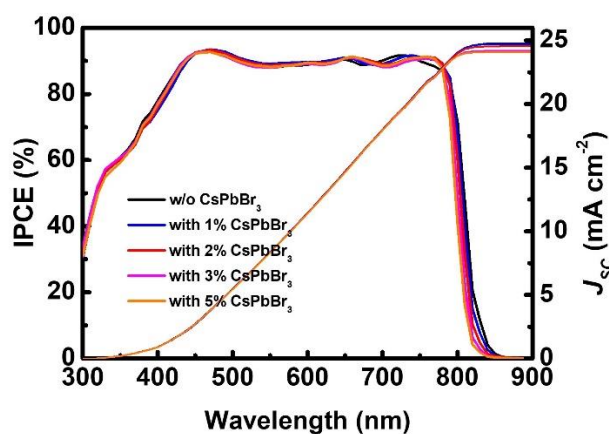


Figure S12. IPCE spectra and integrated  $J_{sc}$  of FAPbI<sub>3</sub>-based PSCs w/o and with CsPbBr<sub>3</sub>.

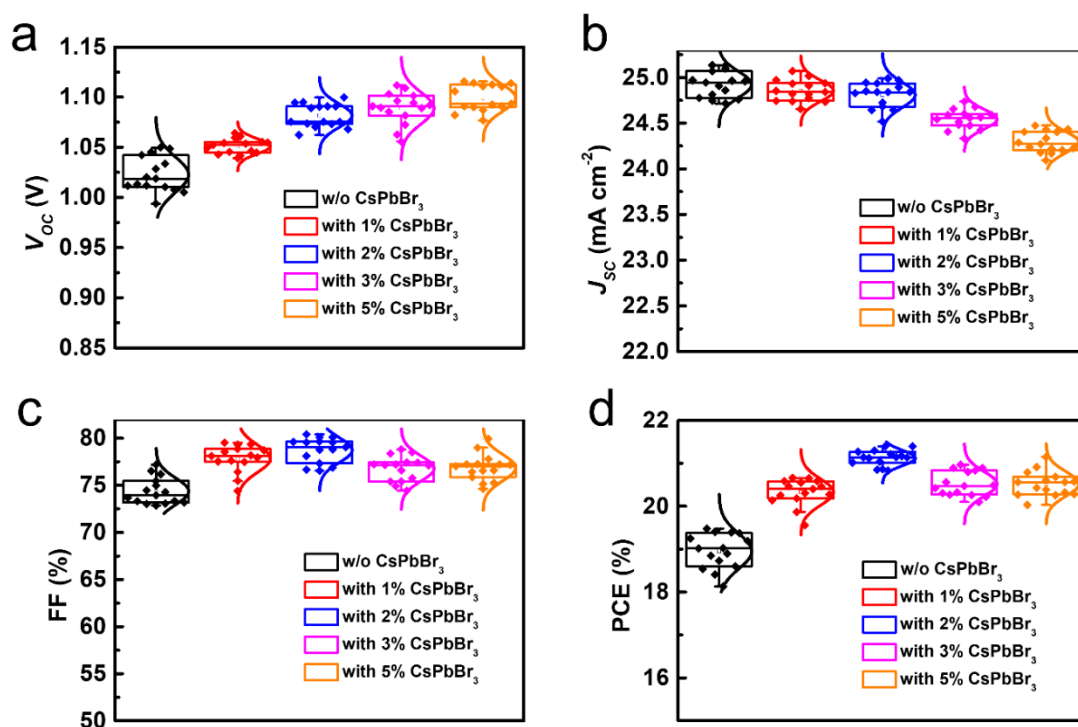


Figure S13. Statistics of photovoltaic metrics of 15 individual FAPbI<sub>3</sub>-based PSCs w/o and with CsPbBr<sub>3</sub>. a)  $V_{oc}$ , b)  $J_{sc}$ , c) FF, and d) PCE.

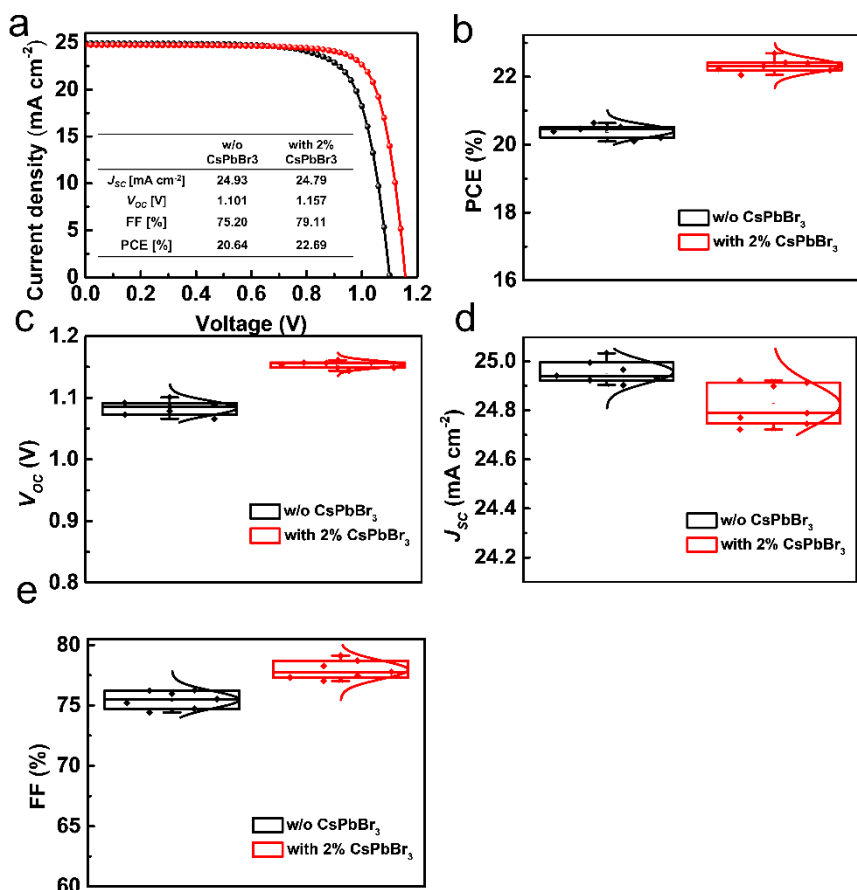


Figure S14. Photovoltaic performance of the FAPbI<sub>3</sub>-based PSCs w/o and with 2% CsPbBr<sub>3</sub> optimized with surface passivation of NMAI. a) *J*-*V* curves. Statistics of b) PCE, c) *V*<sub>oc</sub>, d) *J*<sub>sc</sub>, and e) FF.

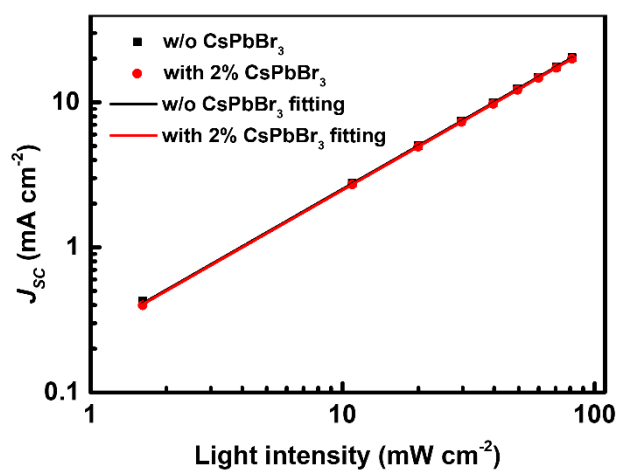


Figure S15. The dependency of *J*<sub>sc</sub> versus illumination intensity of FAPbI<sub>3</sub>-based PSCs w/o and with 2% CsPbBr<sub>3</sub>.

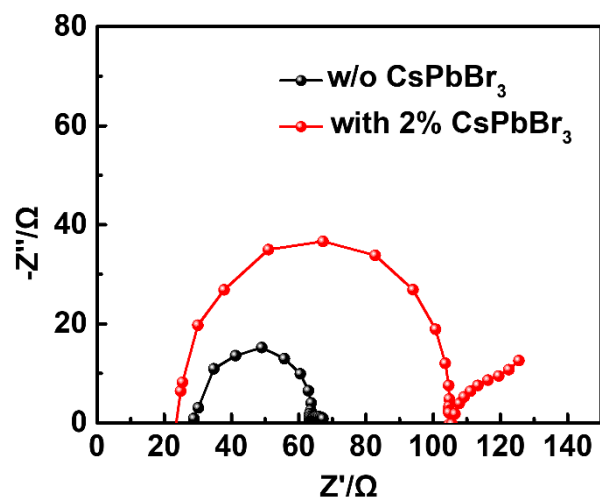


Figure S16. EIS of FAPbI<sub>3</sub>-based PSCs w/o and with 2% CsPbBr<sub>3</sub>. The applied bias was 1 V (close to the open circuit) and the illumination intensity was 10 mW cm<sup>-2</sup> (0.1 sun). These testing conditions were employed to emphasize the recombination characteristics.

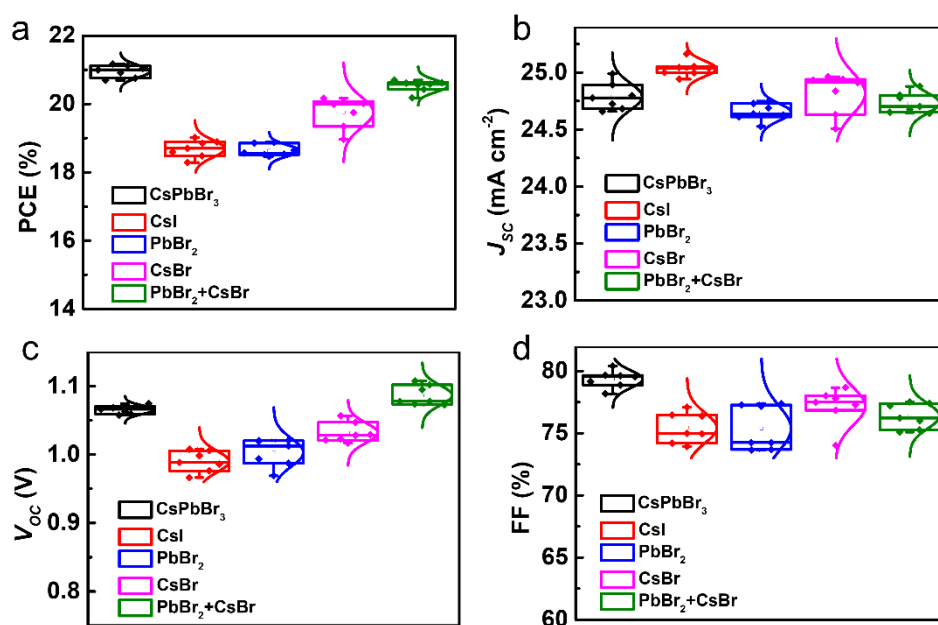


Figure S17. Photovoltaic metrics statistics of FAPbI<sub>3</sub>-based PSCs stabilized with perovskite-type stabilizer (CsPbBr<sub>3</sub>), precursor-type stabilizers (CsI, PbBr<sub>2</sub>, or CsBr) and corresponding double precursor-type stabilizers (PbBr<sub>2</sub>+CsBr). The relative content of stabilizers are fixed at 2%. a) PCE, b)  $J_{sc}$ , c)  $V_{oc}$ , and d) FF.



Table S1. Fitted parameters of TRPL results of FAPbI<sub>3</sub>-based perovskite films w/o and with CsPbBr<sub>3</sub>.

Devices	w/o CsPbBr <sub>3</sub>	with 1% CsPbBr <sub>3</sub>	with 2% CsPbBr <sub>3</sub>	with 3% CsPbBr <sub>3</sub>	with 5% CsPbBr <sub>3</sub>
$\tau_1$ (ns)	17.8	27.5	61.3	39.5	34
$\tau_2$ (ns)	326.6	359.8	371.7	358	344
A <sub>1</sub>	32.8	7.6	1.0	2.9	4.8
A <sub>2</sub>	0.4	0.3	0.6	0.6	0.3

Table S2. Photovoltaic parameters of FAPbI<sub>3</sub>-based PSCs with CsPbBr<sub>3</sub>.

Devices	$J_{SC}$ [mA cm <sup>-2</sup> ]	$V_{OC}$ [V]	FF [%]	PCE [%]
with 1% CsPbBr <sub>3</sub>	25.01	1.042	78.85	20.54
with 3% CsPbBr <sub>3</sub>	24.58	1.095	77.43	20.83
with 5% CsPbBr <sub>3</sub>	24.20	1.116	76.60	20.68

Table S3. Accuracy of  $J_{SC}$  measured by  $J-V$  curves evaluated by the mismatch between integrated  $J_{SC}$  values from IPCE and extracted  $J_{SC}$  from  $J-V$  curves.

Devices	w/o CsPbBr <sub>3</sub>	with 1% CsPbBr <sub>3</sub>	with 2% CsPbBr <sub>3</sub>	with 3% CsPbBr <sub>3</sub>	with 5% CsPbBr <sub>3</sub>
Integrated $J_{sc}$ (mA cm <sup>-2</sup> )	24.79	24.72	24.55	24.19	24.08
$J_{sc}$ extracted from $J-V$ (mA cm <sup>-2</sup> )	25.12	25.01	24.83	24.58	24.20
Mismatch (%)	1.3	1.2	1.1	1.6	0.5

Table S4. Summary of representative efficiency and stability of FAPbI<sub>3</sub>-based PSCs stabilized with different types of additives reported in the past three years.

Stabilizer	Type	Cs-containing	Champion PCE (%)	Operational stability	Published year	Ref
MACl	Precursor	No	23.48% (Certified)	$T_{90}$ = 300 h @ 40 °C (heat stability)	2019	[1]
MACl	Precursor	No	23.1%	$T_{80}$ = 150 h @ AM 1.5G, N <sub>2</sub> (light stability)	2021	[2]
MAI & MACl	Precursor	No	23.32% (Certified)	$T_{80}$ ≈ 500 h @ 85 °C, N <sub>2</sub> (heat stability)	2019	[3]
MDACl <sub>2</sub> (MDA = <sup>+</sup> H <sub>3</sub> N-CH <sub>2</sub> -NH <sub>3</sub> <sup>+</sup> ) & MACl	Precursor	No	23.7% (Certified)	$T_{90}$ = 600 h @ AM 1.5G in the air with encapsulation (light stability)	2019	[4]
CsI & GAI (GA = HNC(NH <sub>2</sub> ) <sub>2</sub> )	Precursor	Yes	23.5%	$T_{80}$ ≈ 250 h @ 0.8 sun (light stability)	2020	[5]
Cs <sub>0.10</sub> FA <sub>0.78</sub> MA <sub>0.12</sub> PbI <sub>2.55</sub> Br <sub>0.45</sub>	Perovskite	Yes	21.7%	$T_{60}$ = 280 h @ AM 1.5G in N <sub>2</sub> (light stability)	2018	[6]
CsCl & Cs <sub>0.10</sub> FA <sub>0.78</sub> MA <sub>0.12</sub> PbI <sub>2.55</sub> Br <sub>0.45</sub>	Perovskite	Yes	22.1%	$T_{90}$ = 4000 min @ AM 1.5G, N <sub>2</sub> (light stability)	2018	[7]
Cs <sub>0.2</sub> MA <sub>0.2</sub> FA <sub>0.6</sub> Pb(I <sub>0.22</sub> Br <sub>0.78</sub> ) <sub>3</sub>	Perovskite	Yes	21.5%	$T_{80}$ = 500 h @ AM 1.5G, N <sub>2</sub> , (light stability)	2019	[8]
δ-CsPbI <sub>3</sub>	Non-perovskite	Yes	20.45%	$T_{70}$ = 20 min @ AM 1.5G, Air (55%-60% RH) (light stability)	2019	[9]
MAPbBr <sub>3</sub> & MACl	Perovskite	No	22.51%	$T_{97}$ = 2600 h @ dark, 20% RH	2019	[10]
δ-CsPbI <sub>3</sub> & δ-RbPbI <sub>3</sub>	Non-perovskite	Yes	22.30%	$T_{92}$ = 400 h @ AM 1.5G, N <sub>2</sub> , (light stability)	2021	[11]
MAPbBr <sub>3</sub> & MACl	Perovskite	No	25.2% (Certified)	$T_{80}$ = 500 h @ AM 1.5G, 40°C with encapsulation (light stability)	2021	[12]
CsPbBr <sub>3</sub> & MACl & MAI	Perovskite	Yes	23.34%	$T_{80}$ = 1153 h @ AM 1.5G, N <sub>2</sub> , (light stability)	This work	

## References

- 1 M. Kim, G. H. Kim, T. K. Lee, I. W. Choi, H. W. Choi, Y. Jo, Y. J. Yoon, J. W. Kim, J. Lee, D. Huh, H. Lee, S. K. Kwak, J. Y. Kim and D. S. Kim, *Joule*, 2019, **3**, 2179-2192.
- 2 F. Ye, J. Ma, C. Chen, H. Wang, Y. Xu, S. Zhang, T. Wang, C. Tao and G. Fang, *Adv. Mater.*, 2021, **33**, e2007126.
- 3 Q. Jiang, Y. Zhao, X. Zhang, X. Yang, Y. Chen, Z. Chu, Q. Ye, X. Li, Z. Yin and J. You, *Nat. Photon.*, 2019, **13**, 460-466.
- 4 H. Min, M. Kim, S. U. Lee, H. Kim, G. Kim, K. Choi, J. H. Lee and S. I. Seok, *Science*, 2019, **366**, 749-753.
- 5 M. Qin, H. Xue, H. Zhang, H. Hu, K. Liu, Y. Li, Z. Qin, J. Ma, H. Zhu, K. Yan, G. Fang, G. Li, U. S. Jeng, G. Brocks, S. Tao and X. Lu, *Adv. Mater.*, 2020, **32**, e2004630.
- 6 Y. Zhao, H. Tan, H. Yuan, Z. Yang, J. Z. Fan, J. Kim, O. Voznyy, X. Gong, L. N. Quan, C. S. Tan, J. Hofkens, D. Yu, Q. Zhao and E. H. Sargent, *Nat. Commun.*, 2018, **9**, 1607.
- 7 Q. Li, Y. Zhao, R. Fu, W. Zhou, Y. Zhao, X. Liu, D. Yu and Q. Zhao, *Adv. Mater.*, 2018, **30**, e1803095.
- 8 Q. Li, Y. Zhao, W. K. Zhou, Z. Y. Han, R. Fu, F. Lin, D. P. Yu and Q. Zhao, *Adv. Energy Mater.*, 2019, **9**, 1902239.
- 9 S. Wang, J. Jin, Y. Qi, P. Liu, Y. Xia, Y. Jiang, R. X. He, B. Chen, Y. Liu and X. Z. Zhao, *Adv. Funct. Mater.*, 2019, **30**, 1908343.
- 10 G. Yang, H. Zhang, G. Li and G. Fang, *Nano Energy*, 2019, **63**, 103835.
- 11 E. A. Alharbi, T. P. Baumeler, A. Krishna, A. Y. Alyamani, F. T. Eickemeyer, O. Ouellette, L. Pan, F. S. Alghamdi, Z. Wang, M. H. Alotaibi, B. Yang, M. Almalki, M. D. Mensi, H. Albrithen, A. Albadri, A. Hagfeldt, S. M. Zakeeruddin and M. Grätzel, *Adv. Energy Mater.*, 2021, **11**, 2003785.
- 12 J. J. Yoo, G. Seo, M. R. Chua, T. G. Park, Y. Lu, F. Rotermond, Y. K. Kim, C. S. Moon, N. J. Jeon, J. P. Correa-Baena, V. Bulovic, S. S. Shin, M. G. Bawendi and J. Seo, *Nature*, 2021, **590**, 587-593.